

Baryon Resonances without Quarks: a Chiral Soliton Perspective*

MAREK KARLINER

*Stanford Linear Accelerator Center
Stanford University, Stanford, California, 94305*

ABSTRACT

In many processes involving low momentum transfer it is fruitful to regard the nucleon as a soliton or “monopole-like” configuration of the pion field. In particular, within this framework it is possible to obtain detailed predictions for pion-nucleon scattering amplitudes and for properties of baryon resonances. One can also derive model-independent linear relations between scattering amplitudes, such as πN and $\bar{K}N$. A short survey of some recent results is given, including comparison with experimental data.

1. INTRODUCTION

This talk describes the application of chiral soliton ideas to the meson-baryon S -matrix. Most of the original work reported here was done in collaboration with Michael Mattis at SLAC.^[4,8,9]

How can the chiral soliton picture of the nucleon be put to a quantitative test? The flow chart in Fig. 1 illustrates two potentially productive approaches to the problem. Both will be described in some detail in the course of this talk. For now, I will just summarize the two alternatives.

One possibility is to take the simplest realization of this picture, i.e. the simplest mesonic Lagrangian admitting soliton solutions with the right quantum numbers and then calculate the properties of baryons in that model. The simplest model satisfying such criteria is the Skyrme model. In that model the

* Work supported by the Department of Energy, contract DE – AC03 – 76SF00515.

Invited talk presented at the Workshop on Skyrmions and Anomalies, Kraków, Poland, February 20-24, 1987.

pion-nucleon scattering matrix can be computed explicitly and it is in good agreement with experiment. The Skyrme Lagrangian is of course only a very crude approximation to the true low-energy effective Lagrangian of QCD. In addition, the results obtained from the Skyrme model might therefore depend on the details of the action. Hence the second approach for testing the chiral soliton picture:

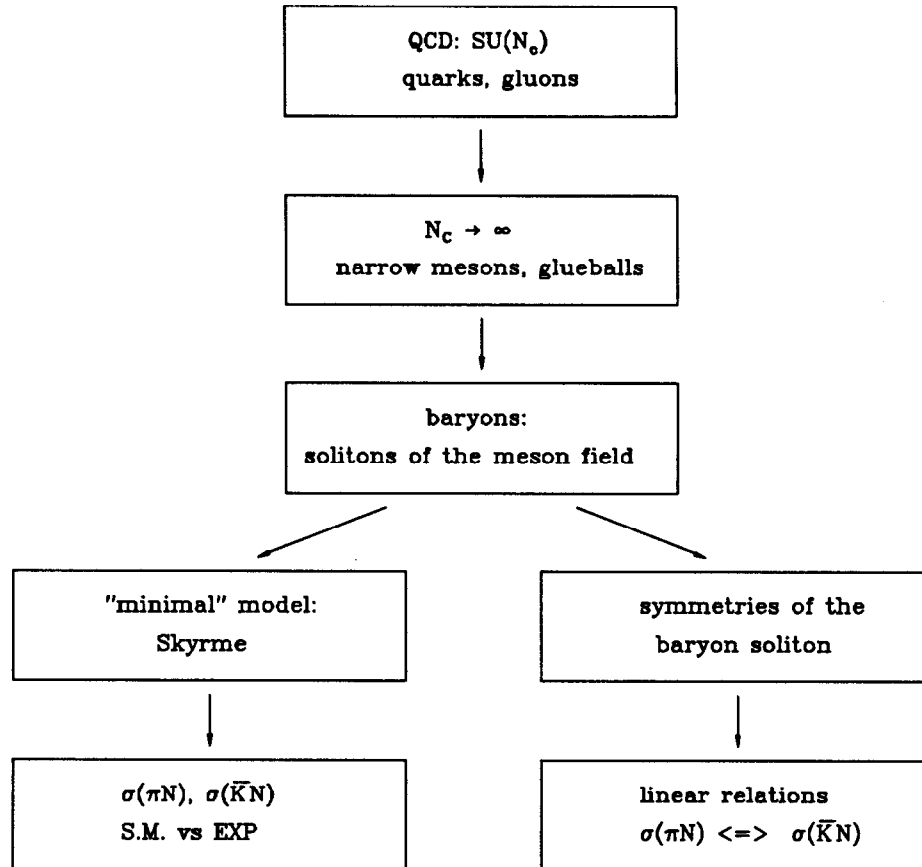


Fig. 1. Flow chart illustrating two possible ways of putting the chiral soliton ideas to a quantitative test: a model-dependent and a model-independent one.

it turns out that one can derive model independent predictions, valid for all models in which the baryon corresponds to a soliton of a hedgehog form. In all such models the static soliton is not an eigenstate of the isospin \mathbf{I} , nor of the angular momentum \mathbf{L} . Instead it is invariant under the action of $\mathbf{K} = \mathbf{I} + \mathbf{L}$. Therefore the meson-baryon S -matrix has well-defined transformation properties under \mathbf{K} . This property of the S -matrix yields new and somewhat surprising relations between the various meson-baryon scattering matrix elements. Some of these model-independent relations are satisfied remarkably well in Nature. Let

me now describe the two approaches in some detail, addressing first the Skyrme model calculation. I will begin with a very brief review of some basic results in Ref. 3. The Skyrme Lagrangian with a chiral-symmetry breaking mass-term is given by

$$\mathcal{L} = \frac{f_\pi^2}{16} \text{Tr} \left(\partial_\mu U \partial_\mu U^\dagger \right) + \frac{1}{32e^2} \text{Tr} \left[(\partial_\mu U) U^\dagger, (\partial_\nu U) U^\dagger \right]^2 + \frac{f_\pi^2 m_\pi^2}{8} (\text{Tr} U - 2). \quad (1)$$

Here f_π is the pion decay constant (186 MeV in the real world), m_π is the pion mass, and e is a new, dimensionless coupling constant peculiar to the model. The “small parameter” $1/N$ enters the Lagrangian through f_π and e , which behave like $N^{\frac{1}{2}}$ and $N^{-\frac{1}{2}}$ in the large- N limit, respectively.

The chirally invariant vacuum is $U(x) \equiv 1$ and pions are usually thought of as small fluctuations around this state, hence the standard notation:

$$U = \exp \left[\frac{2i}{f_\pi} \vec{\pi}(\vec{x}, t) \cdot \vec{\tau} \right]$$

For small $\vec{\pi}/f_\pi$ we have $U \approx 1 + 2i\vec{\pi}(\vec{x}, t) \cdot \vec{\tau}/f_\pi$ and then the first term in Eq. (1) becomes just the kinetic term for free pions, as expected:

$$\frac{f_\pi^2}{16} \text{Tr} \left(\partial_\mu U \partial_\mu U^\dagger \right) \rightarrow \frac{1}{2} (\partial_\mu \vec{\pi} \cdot \partial_\mu \vec{\pi}) + \dots \quad (2)$$

In addition to the vacuum solution, (1) has static soliton solutions which break the chiral symmetry and carry one unit of baryon number. They can all be obtained by an isospin rotation from the canonical “hedgehog” solution:

$$U_0 = \exp [F(\mathbf{r}) \hat{\mathbf{r}} \cdot \vec{\tau}] \quad (3)$$

$$U_A = A U_0 A^{-1}$$

where A is a constant $SU(2)$ matrix. When A is treated as a collective coordinate, one finds that the nucleon corresponds to a superposition of the U_A -s. Schematically we can write this as

$$|N\rangle = \int dA \chi(A) |A\rangle$$

where $\chi(A)$ is the wave-function in the space of collective coordinates. While $|A\rangle$ corresponds to a state pointing in a well-defined direction in the internal space, it has an ill-defined isospin and angular momentum. On the other hand, the state $|N\rangle$ has well-defined spin and isospin, but does not point in any specific direction in the internal space. The situation here is completely analogous to the problem of a particle constrained to move on a circular ring, as shown in Fig. 2.

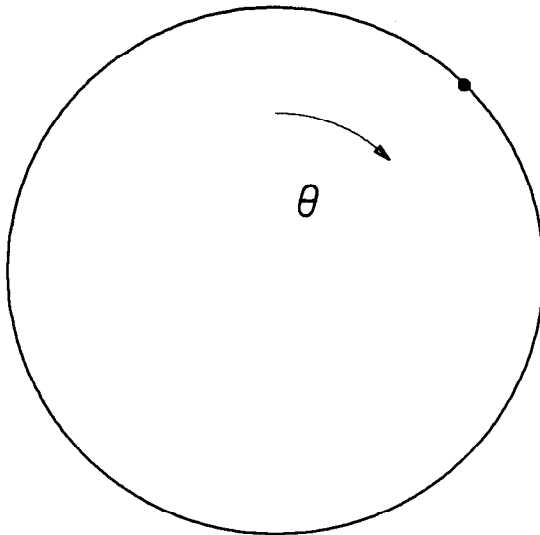


Fig. 2. A one-dimensional analogue of the collective coordinate A : particle constrained to move on a circular ring. Classical ground state corresponds to a particle at rest at some fixed angle θ . In quantum mechanics this is no longer true and we must have an eigenstate of the angular momentum operator $L_\theta = -i\frac{\partial}{\partial\theta}$.

Classically, a particle at rest at any angle θ is a ground state of the system. In quantum mechanics the eigenstates of the hamiltonian no longer are localized at a fixed angle θ . Instead, they are eigenstates of the angular momentum operator $L_\theta = -i\frac{\partial}{\partial\theta}$. Using this analogy, we see that a nucleon with a well-defined spin and isospin corresponds to a *rotating soliton*.

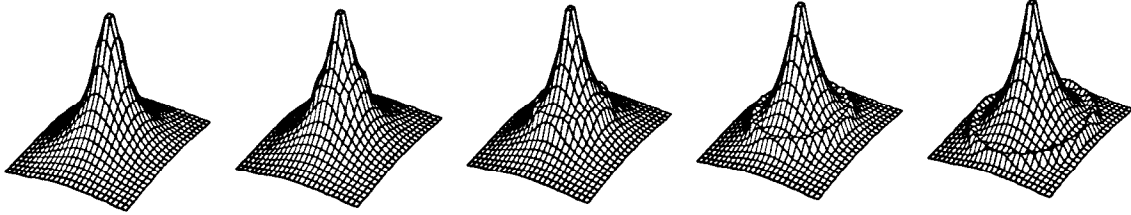
Static properties of the nucleon in the Skyrme model obtained in Ref. 3 were based on treating f_π and e as free parameters, to be adjusted for the best fit to nucleon and Δ masses. All other static quantities were obtained as functions of e and f_π . Some properties of the nucleon turned out very well, but some others were in serious disagreement with experiment. Most notably, the values of f_π and g_A had errors of about 30% and 50%, respectively. At this point it is worth reminding ourselves that the Skyrme Lagrangian is in principle an equally good approximation to an underlying $SU(N)$ gauge theory with $N = 3$ or $N = 5$, etc. In the real world $N = 3$ and it is therefore very unlikely that the Skyrme Lagrangian can reproduce experimental quantities which explicitly depend on N . Typically the most we can hope for is to reproduce experimental quantities which do not depend on N in the leading order of the $1/N$ expansion. For example, while $f_\pi \sim N^{\frac{1}{2}}$ and $g_A \sim N$, the ratio $f_\pi^2/g_A \sim N^0$ and in contrast to f_π and g_A taken separately, it reproduces experiment to 3%. As shown in Table I, similar statements can be made about some other N -independent ratios.

TABLE I
 STATIC PROPERTIES OF THE NUCLEON IN THE SKYRME MODEL
 AND THEIR DEPENDENCE ON N .

Quantity	N -dependence	Prediction	Experiment	Error
$\langle r^2 \rangle_{I=0}^{1/2}$	$\sim N^0$	0.59 fm	0.72 fm	18%
$\langle r^2 \rangle_{M,I=0}^{1/2}$	$\sim N^0$	0.92 fm	0.81 fm	14%
μ_p	$\sim N$	1.87	2.79	33%
μ_n	$\sim N$	-1.31	-1.91	31%
μ_p/μ_n	$\sim N^0$	1.43	1.46	2%
g_Λ	$\sim N$	0.61	1.23	50%
f_π	$\sim N^{1/2}$	129 MeV	186 MeV	31%
f_π^2/g_Λ	$\sim N^0$	27,280 MeV ²	28,127 MeV ²	3%
$g_{\pi NN}$	$\sim N^{3/2}$	8.9	13.5	34%
$g_{\pi N\Delta}$	$\sim N^{3/2}$	13.2	20.3	35%
$g_{\pi N\Delta}/g_{\pi NN}$	$\sim N^0$	1.5	1.5	$\lesssim 1\%$

The predictions are from Ref. 3. Skyrme model is *a priori* an equally good effective Lagrangian for $N_c = 3$ and $N_c = 5$. So it does not reproduce well the quantities which depend on N in the leading order of the $1/N$ expansion. On the other hand, as demonstrated by the table above, it typically does much better for ratios in which the N -dependence cancels out.

The purpose of this example is *not* to suggest that *all* N -independent quantities should agree well with experiment, for this is hardly the case. The results in Table I suggest however that the N -independent quantities stand a better chance of reproducing the real world data. If our guiding principle is to look for such quantities, it is natural to examine the pion-nucleon S -matrix, since meson-



$$U_0 = \exp [F(\mathbf{r})\hat{\mathbf{r}} \cdot \vec{\tau}]$$

$$U = \exp \left[F(\mathbf{r})\hat{\mathbf{r}} \cdot \vec{\tau} + \frac{2i\vec{\pi}(\vec{x}, t)}{f_\pi} \right]$$

Fig. 3. A two-dimensional example showing how fluctuations around the classical soliton profile should be identified with the physical mesons. Time flows from left to right and the fluctuation corresponds to an outgoing spherical wave.

baryon scattering amplitudes are independent of N in the large- N limit^[1].

The first step towards the computation of the πN S -matrix is the realization that small fluctuations around the soliton can be identified with physical mesons. This is schematically illustrated in Fig. 3.*

Once that identification is made, it is clear that in order to obtain the pion-nucleon S -matrix, we should in principle find the eigenmodes of small fluctuations around a rotating soliton. This is a very difficult problem. Fortunately enough, in the large- N limit there is an important simplification: in that limit the soliton rotates very slowly, with angular velocity $\omega_s \sim 1/N$. The reason is as follows. The spin of the nucleon is $\frac{1}{2}\hbar$, independent of N . It is the product of the Skyrmion angular velocity ω_s and its moment of inertia I_s . The Skyrmion

* This identification breaks down for fluctuations which do not change the energy of the system. Such fluctuations correspond to the translational and rotational zero modes of the soliton. In our treatment this subtlety is neglected, spoiling the agreement with experiment in the low partial waves.

radius R_s is independent of N and its mass M_s scales like N .^[1] Consequently

$$I_s \sim M_s R_s^2 \sim N \quad \text{while} \quad I_s \omega_s = \frac{1}{2} \hbar \sim N^0$$

therefore

$$\omega_s \sim 1/N$$

The characteristic time scale t_{rot} associated with the Skyrmion rotation is large, $t_{rot} \sim 1/\omega_s \sim N$. It is much greater than the time t_π that a pion moving with the speed of light spends in the vicinity of the nucleon:

$$R_s \sim N^0; \quad R_s/c \sim N^0 \sim t_\pi \ll t_{rot} \sim N$$

A pion will therefore not observe the rotation, but rather will take a “snapshot” of the soliton in one of its possible orientations. The probability of any given orientation is proportional to $|\chi(A)|^2$. This justifies the impulse approximation: first obtaining the scattering amplitude for scattering of a pion by a soliton *pointing in a fixed orientation* and then superimposing such amplitudes, according to their weight in $\chi(A)$.

In addition to neglecting the rotation, as described above, we can neglect the nucleon recoil, since in the large- N limit the pion kinetic energy in the domain of interest is independent on N , while $M_s \sim N$. In order to obtain the Lagrangian describing scattering of mesons by a static soliton, we write the chiral field U in the form:

$$U = \exp \left[F(\mathbf{r}) \hat{\mathbf{r}} \cdot \vec{\pi} + \frac{2i\vec{\pi}}{f_\pi} \right]. \quad (4)$$

This form of U is then plugged back into the original Lagrangian (1) and the action is expanded in powers of $\vec{\pi}/f_\pi$:

$$\mathcal{L}(U) \rightarrow \mathcal{L}(\vec{\pi}) = \frac{1}{2} \vec{\pi} \mathbb{L} \vec{\pi} + \mathcal{O}(\vec{\pi}^3/f_\pi^3) \quad (5)$$

where \mathbb{L} is a second-order linear differential operator depending on U_0 . For $r \rightarrow \infty$, $U_0 \rightarrow 1$ and then \mathbb{L} becomes just the free four-Laplacian, as in (2). The term linear in $\vec{\pi}$ vanishes, since U_0 is an extremum of the classical action. In addition, in the $N \rightarrow \infty$ limit we can formally neglect the $\mathcal{O}(\vec{\pi}^3/f_\pi^3)$ terms, since $f_\pi \sim N^{1/2}$, and such terms are suppressed relative to the quadratic one. We are

left with a quadratic Lagrangian and therefore with linear equations of motion, which can be schematically written as:

$$\mathbb{L}\vec{\pi} = 0 \quad .$$

These equations describe the motion of a meson in a potential provided by the soliton background.[†] Since the potential is invariant under \mathbf{K} , K plays the role of the angular momentum in the usual partial wave decomposition. The equations can be explicitly solved for each value of K , yielding the eigenmodes of $\vec{\pi}$ as functions of energy. For $|\vec{x}| \gg R_s$, $F(r) \rightarrow 0$ (cf. Eq. (3)), the potential vanishes, and up to a phase, the $\vec{\pi}$ wave function is that of a free particle. This phase is just the scattering phase-shift defining the S -matrix element in a given pion-Skyrmion channel. We shall refer to the latter as *reduced* matrix elements. The reason for this name will become clear in a moment.

In order to obtain the pion-nucleon S -matrix from the pion-Skyrmion one, we need to project the Skyrmion onto states with well-defined isospin and spin. This projection is carried out as follows. First, given the T-matrix^{*} T_{U_0} for scattering off U_0 , the corresponding T-matrix for scattering off U_A (cf. Eq. (3)) is given by:

$$T_{U_A} = \hat{D}(A) T_{U_0} \hat{D}(A)^\dagger \quad (6)$$

where \hat{D} is the adjoint representation of A . Next we superimpose the T_{U_A} -s according to their weight in the nucleon wave function $\chi(A)$. The complete expression for the physical T-matrix is then:

$$T_{PHYS} = \int_{SU(N_f)} dA \chi_f^\dagger(A) \hat{D}(A) T_{U_0} \hat{D}(A)^\dagger \chi_i(A) \quad (7)$$

where $SU(N_f)$ is the flavor group and $\chi_{i(f)}$ is the wave function of the baryon in the initial (final) state. Integration over the flavor group can be carried out in closed form (see Appendix B of Ref. 9 for details.) The final result has a very simple structure:

$$T_{PHYS} = \sum_i C_i \tau_i^{\text{RED}} \quad (8)$$

where τ^{RED} are the T-matrix elements in the pion-Skyrmion system and the C_i -s are group-theoretical factors. The structure of Eq. (8) explicitly demon-

[†] The explicit expression for \mathbb{L} is rather complicated and will not be given here. Interested reader is referred to the original literature Refs. 4, 6, 8 and 9.

^{*} We interchange freely between the S -matrix and T-matrix, using the one which is the most convenient. The two are related by $\mathbf{T} = (\mathbf{S} - 1)/2i$.

states two ingredients on which the physical answer depends: symmetry and dynamics. C_i -s reflect only the symmetry and are independent of the details of the Lagrangian. They are determined by the flavor group and by the fact that the soliton is invariant under \mathbf{K} ; all dynamics is contained in the reduced matrix elements. We are all familiar with this type of division into group theory and dynamics. For example, isospin conservation dictates that the T-matrix for $\pi N \rightarrow \pi N$ is given by

$$T_{\pi N} = C_{\frac{1}{2}} T_{\frac{1}{2}} + C_{\frac{3}{2}} T_{\frac{3}{2}} \quad (9)$$

where $C_{\frac{1}{2}(\frac{3}{2})}$ are $SU(2)$ Clebsch-Gordan coefficients and $T_{\frac{1}{2}(\frac{3}{2})}$ are the $I = \frac{1}{2}(\frac{3}{2})$ reduced matrix elements.

In the foregoing discussion we have focused on the 2-flavor Skyrme model. Extension to 3-flavors is in principle straightforward. The embedding of the $SU(2)$ hedgehog inside $SU(3)$ is done by setting

$$U_0 \rightarrow \left(\begin{array}{c|c} U_0 & \\ \hline & 1 \end{array} \right) \quad (10)$$

Technical details for $SU(3)$ are however much more complicated. The interested reader is again referred to the original literature, especially Ref. 9.

At this point we can summarize the prescription for computing the meson-baryon S -matrix in the Skyrme model:

- identify small fluctuations around the soliton with mesons
- meson wave function \implies phase shifts, τ_i^{RED}
- \mathbf{K} symmetry $\implies T_{\text{PHYS}} = \sum_i C_i \tau_i^{\text{RED}}$
- Approximations:
 - ▷ $m_u = m_d = m_s = 0 \implies$ massless pseudoscalar mesons, exact $SU(3)_f$
 - ▷ Large- $N \implies$ no recoil, linear eq's of motions
 - ▷ Zero modes for $L = 0, 1, 2$; neglected

We are ready to compare the Skyrme model T-matrix with the experiment. It is customary to decompose the experimental data into channels with well-defined isospin I , angular momentum J and orbital angular momentum L . Such channels are denoted by $L_{2I,2J}$ where L is denoted by an appropriate letter: S, P, D, F, G, H, I, K for $L = 0, 1, 2, 3, 4, 5, 6, 7$, respectively. The T-matrix for each $L_{2I,2J}$ channel is plotted as a function of the energy, on the so-called Argand plots (*cf.* Fig. 4).

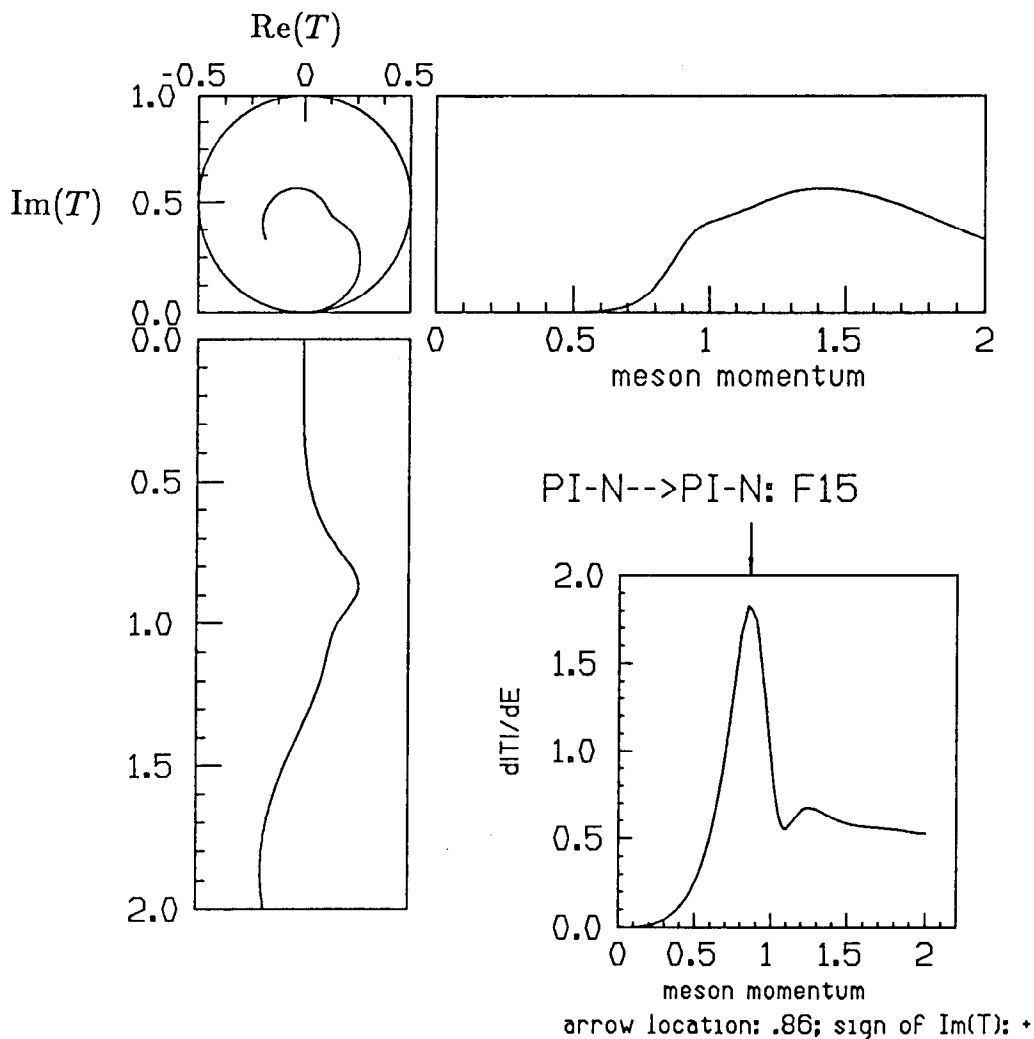


Fig. 4. Sample Argand diagram. A resonance corresponds to the maximum velocity of $d|T|/dE$ (here denoted by an arrow). In the Skyrme model the plot in the unitarity circle, $\text{Im}T$ vs. $\text{Re}T$, is independent of e and f_π .

The part of the diagram bounded by the unitarity circle, $\text{Im}T$ vs. $\text{Re}T$ is independent of e and f_π and therefore provides the most stringent test of the model. Fig. 5 compares the experimental results for $\pi N \rightarrow \pi N$ S -matrix with those of the 3-flavor Skyrme model.

I'd like to stress again that the Skyrme model calculation as shown in Fig. 5 contains no adjustable parameters. The parameters of the model determine the energy scale, but not the shape of the Argand plots. Apart from the S , P and D partial waves, containing the spurious zero modes, overall agreement with

$$\pi N \rightarrow \pi N$$

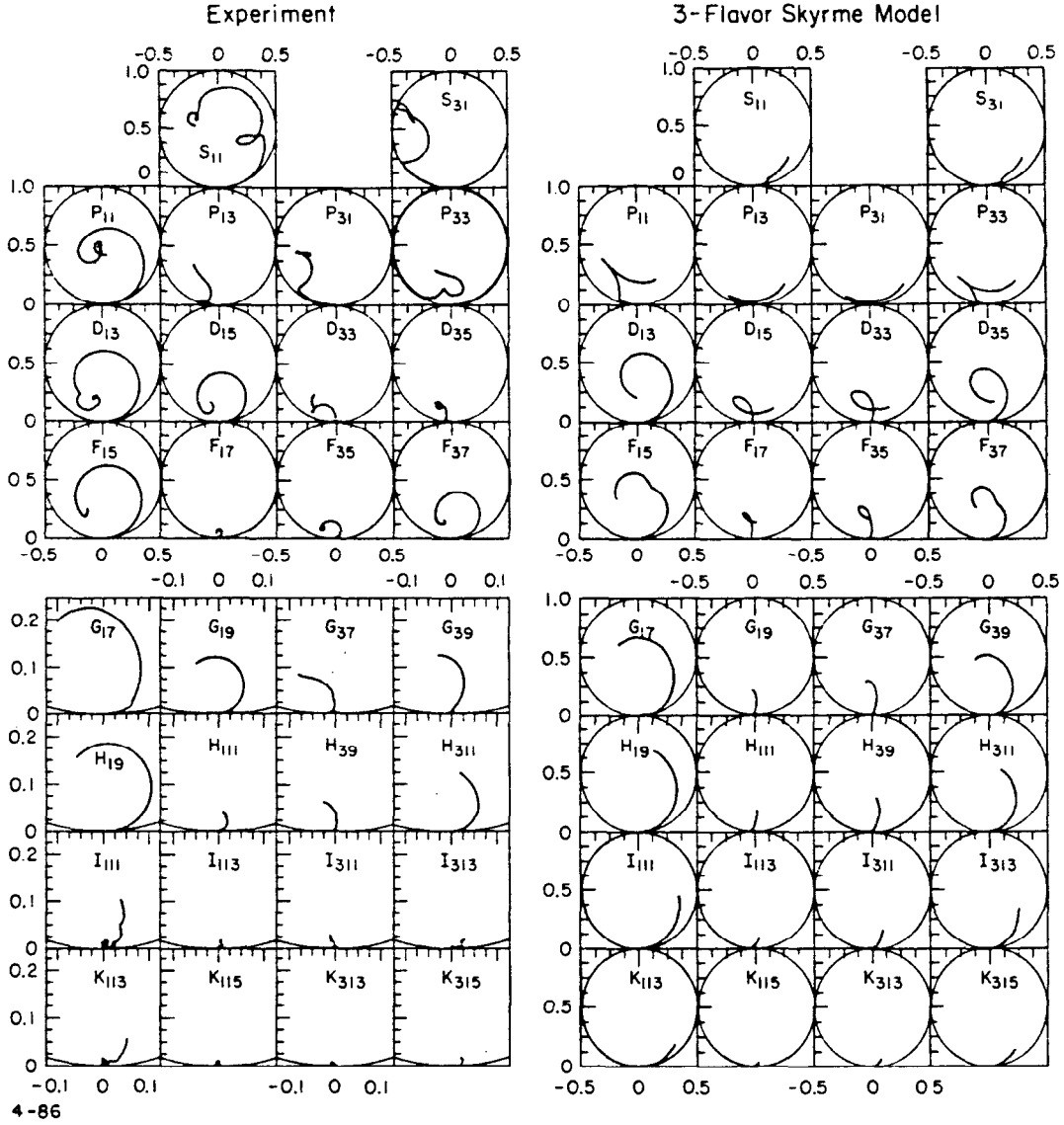


Fig. 5. $\pi N \rightarrow \pi N$: comparison between the 3-flavor Skyrme model and experiment (from Ref. 9). The plots show $\text{Im}(T)$ vs. $\text{Re}(T)$ for each channel. Channels are labeled by L_{2I2J} , where L is the pion orbital angular momentum, I is the total isospin and J the total angular momentum.

experiment is quite good.

The most conspicuous feature of Fig. 5 is the fact that the $L_{I=1/2, J=L-1/2}$ channel is much larger than $L_{I=1/2, J=L+1/2}$ for all L 's. This is true for both experiment and the Skyrme model. A similar, albeit less pronounced pattern holds

for $L_I=3/2, J=L+1/2$ and $L_I=3/2, J=L-1/2$ channels. In the chiral soliton framework this phenomenon has a very simple explanation: there are eight reduced amplitudes entering Eq. (8) for $SU(3)_f$. Out of these, five turn out to be very small and only three are significant, with roughly the same magnitude. The magnitude of the *physical* amplitudes is therefore determined by group theory, *i.e.* the relative strength of the C_i -s multiplying the three principal reduced amplitudes.

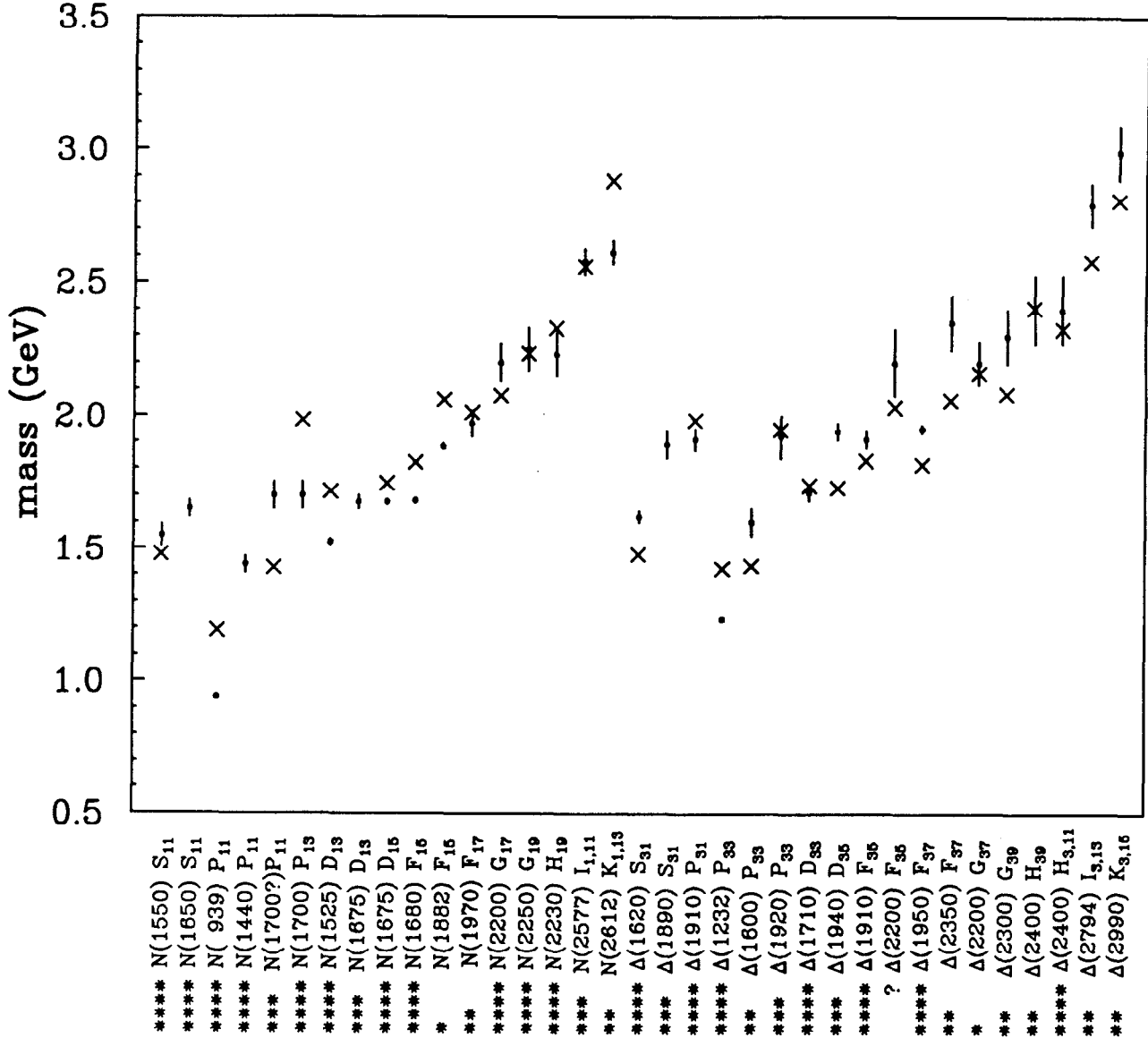


Fig. 6. Spectrum of N and Δ resonances: 3-flavor Skyrme model (crosses) *vs.* experiment (points with error bars) (from Ref. 9). Resonances are assigned stars according to the Particle Data Book. The Skyrme-model values for m_N and m_Δ are obtained from Eq. (9) of Ref. 3, using the “best fit” parameters of Ref. 9 ($e=4.79$, $f_\pi=150$ MeV.)

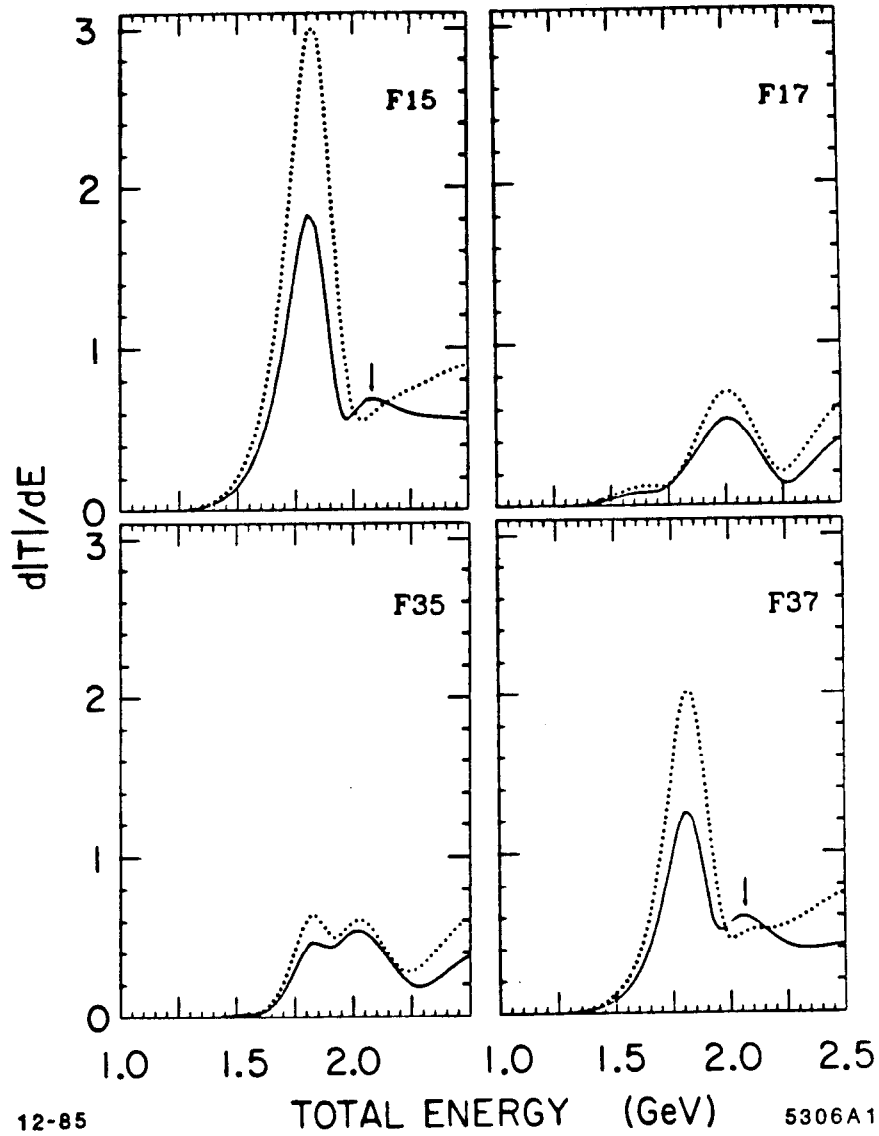


Fig. 7. Speed diagrams for the four F -wave amplitudes in the 2- and 3-flavor Skyrme models (dotted and solid lines, respectively).

Having obtained the complete set of partial-wave channels, we can compute the resonance masses from the maxima of $d|T|/dE$. The resulting spectrum of N and Δ resonances is displayed in Fig. 6. With over 30 resonances and two adjustable parameters, masses are predicted with an average of about 7%. While all of the 4-star resonances appear in the same place in 2- and 3-flavor calculation, the 1- and 2-star resonances in the F_{15} and F_{37} channels supply a

surprise: as demonstrated by Fig. 7, these weak resonances appear only when the third flavor is introduced. It is somewhat puzzling that the appearance of non-strange resonances should be sensitive to the existence of the strange quark. A possible explanation is that they couple to the strange quark sea in the proton.

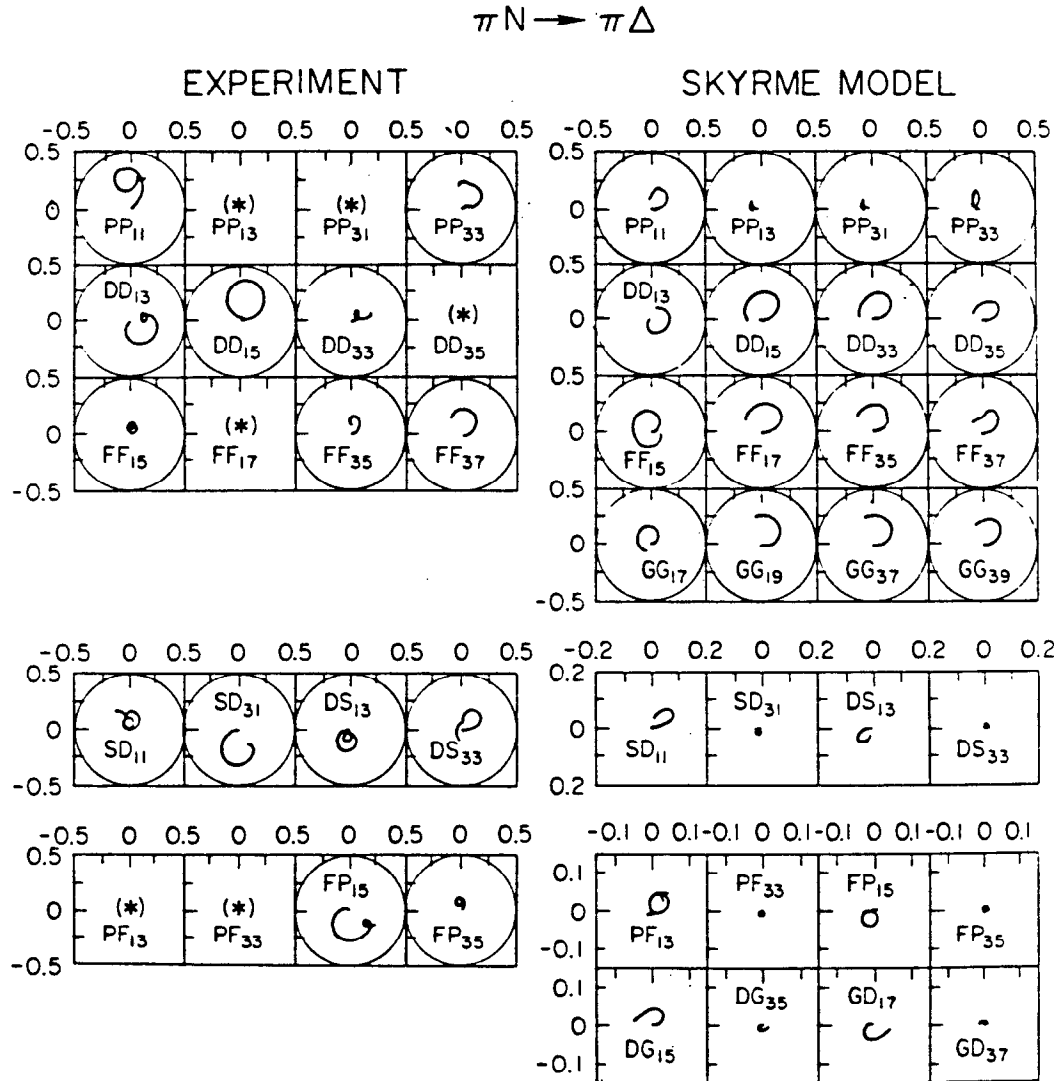


Fig. 8. $\pi N \rightarrow \pi \Delta$: comparison between the 3-flavor Skyrme model and the experimental solution of Ref. 13 (from Ref. 9). Channels are labeled by $LL'_{2I,2J}$, with L and L' the incoming and outgoing pion angular momenta, respectively. An asterisk denotes amplitudes which were found to be small and/or poorly determined by the available data, and were therefore not included in the experimental solution. The partial-wave analysis of the experimental data is not as unambiguous as in $\pi N \rightarrow \pi N$, but in all cases the Skyrme model correctly reproduces the sign of $\text{Im}(T)$, which is a crucial test for theory.

9

In addition to the elastic $\pi N \rightarrow \pi N$ processes, we can also consider inelastic processes, such as $\pi N \rightarrow \pi \Delta$. The only change with respect to $\pi N \rightarrow \pi N$ is that χ_f stands now for the Δ , instead of the nucleon wavefunction. The results are shown in Fig. 8. The experimental partial-wave analysis of $\pi N \rightarrow \pi \Delta$ is somewhat less clear-cut than $\pi N \rightarrow \pi N$, since a $N\pi\pi$ final state may represent $N\rho$, as well as $\Delta\pi$. The sign of $\text{Im}(T)$ is however unambiguous in most cases and wherever it is known experimentally, the Skyrme model yields the correct answer. This is highly non-trivial: the only other theoretical scheme which passes this test is the quark model.

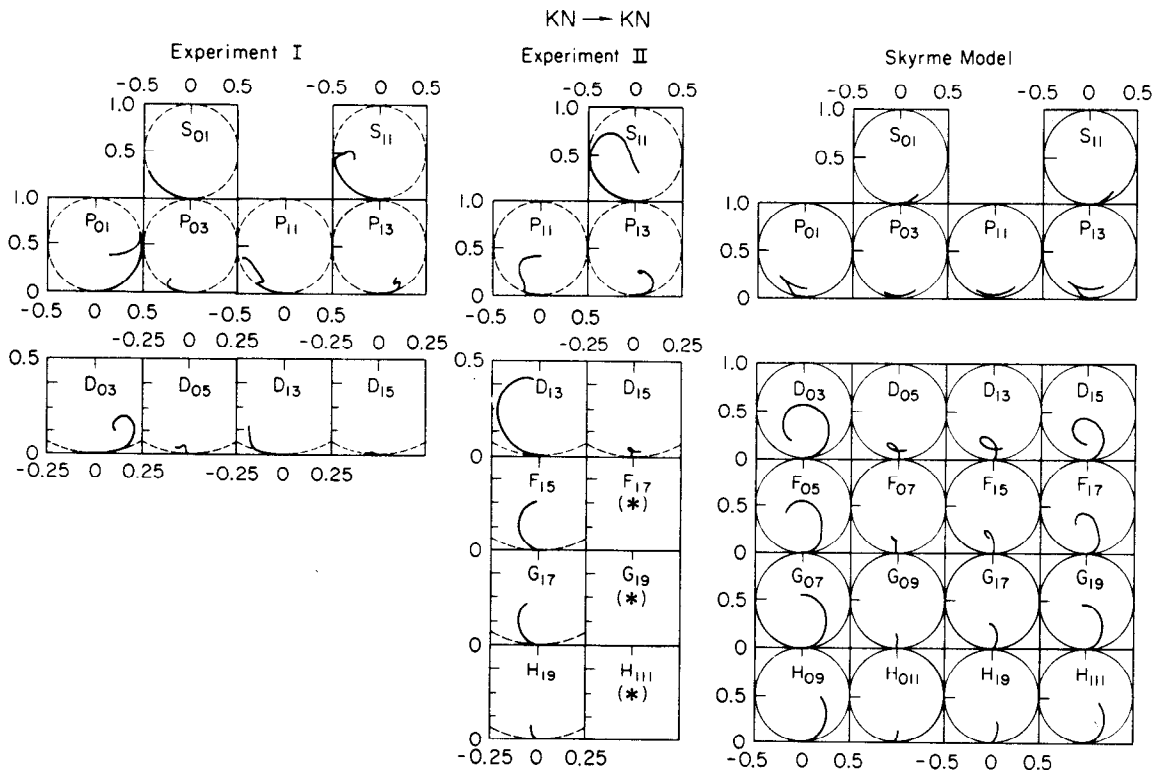


Fig. 9. $KN \rightarrow KN$: comparison between the Skyrme model and two experimental solutions (from Ref. 9): "Experiment I" from Ref. 14 and "Experiment II" from Ref. 15. Channels are labeled by $L_{I,2J}$. Note that experimental and Skyrme-model plots for $L \geq 2$ are shown on different scales. The resonance-like behavior in some of the experimental channels is evident.

The results discussed so far were obtained in the 3-flavor model, but did not involve strange particles. We will now review two processes with open strangeness, beginning with $KN \rightarrow KN$. That reaction is rather different from

$\pi N \rightarrow \pi N$, because any resonances in the KN channels must be exotics, involving more than three quarks. The question whether such resonances exist experimentally has long been a controversial subject.* The Skyrme model has no built-in bias of this kind and therefore it is interesting to compare its predictions with experiment, as shown in Fig. 9. In general, the predictions contain *too many* resonances, compared to the data. Of particular interest are the F -waves, where the model typically works best. The theory predicts a clean resonance in the F_{05} channel, similar to the one observed in D_{03} . This channel has not yet been analyzed experimentally and thus provides an interesting prediction.

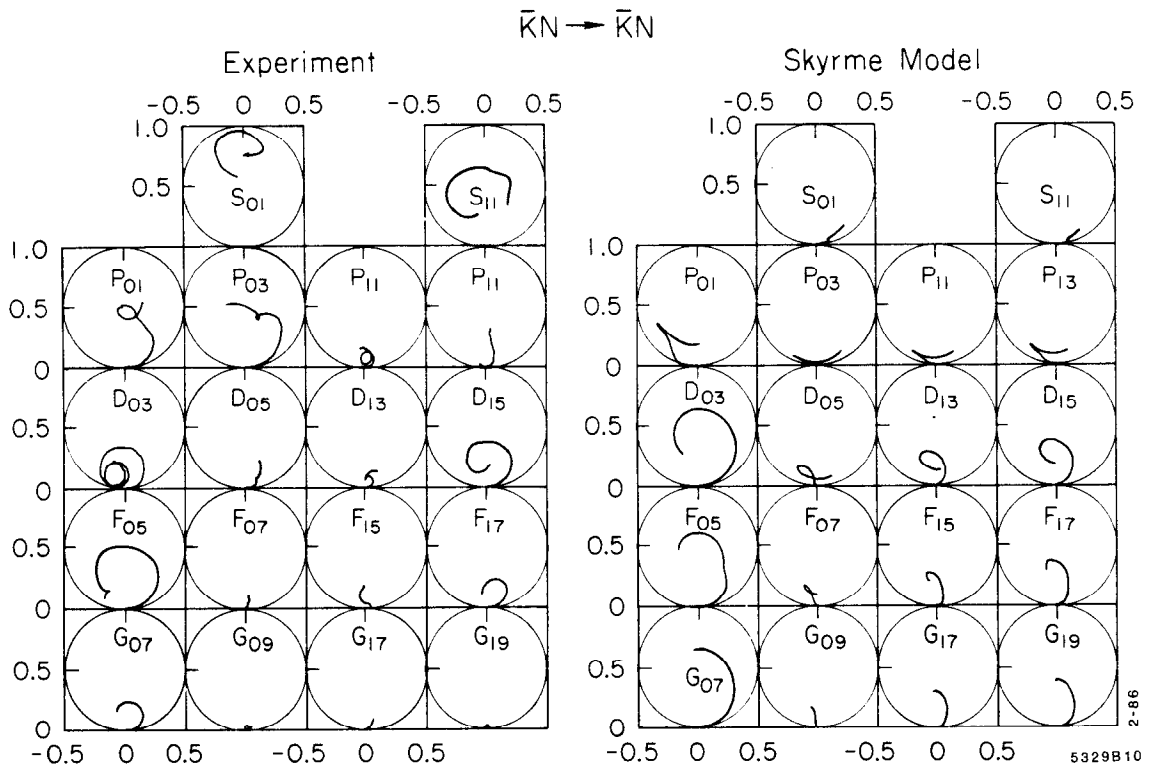


Fig. 10. $\bar{K}N \rightarrow \bar{K}N$: comparison between the Skyrme model and the experimental solution of Ref. 16 (from Ref. 9). Channels are labeled by $L_{l,2J}$.

* Some of our colleagues even refuse to be confused by data, as is perhaps best illustrated by the 1984 Particle Data Book: "... The general feeling, supported by prejudice against baryons not made up of three quarks, is that the suggestive counterclockwise movement in the Argand diagram of some of the partial waves is not real evidence for true Breit-Wigner resonances..." (p. S243)

Contrary to the KN channel, there is nothing exotic about $\overline{KN} \rightarrow \overline{KN}$. The partial-wave analysis of experimental data is of good quality, although not as precise as $\pi N \rightarrow \pi N$, especially in the higher partial waves. The theory reproduces most of the essential features of the experiment, as shown in Fig. 10. Since we work in the chiral limit, $m_K = 0$, there is no point in attempting to extract the spectrum of the strange resonances.

It is possible to study many more inelastic, strange and non-strange processes. Details may be found in Ref. 9. At this point I would however like to move on to the model-independent tests of the chiral soliton picture, as outlined at the beginning of this talk. Let me invoke the isospin analogue once more. If we consider elastic scattering of charged pions on nucleon, *a priori* there are *four* different amplitudes to consider: $T(\pi^+p)$, $T(\pi^-p)$, $T(\pi^+n)$ and $T(\pi^-n)$. From Eq. (9) we learn that they can all be obtained from *two* reduced amplitudes:

$$T_{\pi N} = C_{\frac{1}{2}} T_{\frac{1}{2}} + C_{\frac{3}{2}} T_{\frac{3}{2}}$$

Only two out of the four can be independent, and so there is a *linear relation* between any three of the four. This is a rather generic phenomenon, with an interesting counterpart in the chiral soliton framework, valid for all models in which the nucleon corresponds to a soliton invariant under the \mathbf{K} symmetry: with three flavors any elastic meson-baryon T-matrix element is given by a linear superposition of the eight reduced amplitudes. In the Skyrme model five reduced amplitudes are negligible and the other three make the dominant and roughly equal contributions to the physical amplitudes. Even though we cannot compute the reduced amplitudes in Nature, it is natural to make the dynamical assumption that this hierarchy exists in the real world as well:

$$T_{PHYS} \approx \sum_{i=1}^3 C_i \tau_i^{\text{RED}} \quad (11)$$

Such an assumption not only explains why for $\pi N \rightarrow \pi N$ $L_{I=1/2, J=L-1/2} \gtrsim L_{I=1/2, J=L-1/2}$, etc., but also yields some quite new and interesting predictions. For a given value of L there are many experimental amplitudes, all determined in terms of the three unknown reduced amplitudes. Consequently, there are linear relations among the experimental amplitudes. Such relations are almost model independent, relying only on the K -symmetry group theory and on the assumption that scattering is dominated by the three reduced amplitudes.

First, there are rather accurate linear relations between $\pi N \rightarrow \pi N$ and $\pi N \rightarrow \pi \Delta$. Very similar relations can be derived in the 2-flavor case, as was

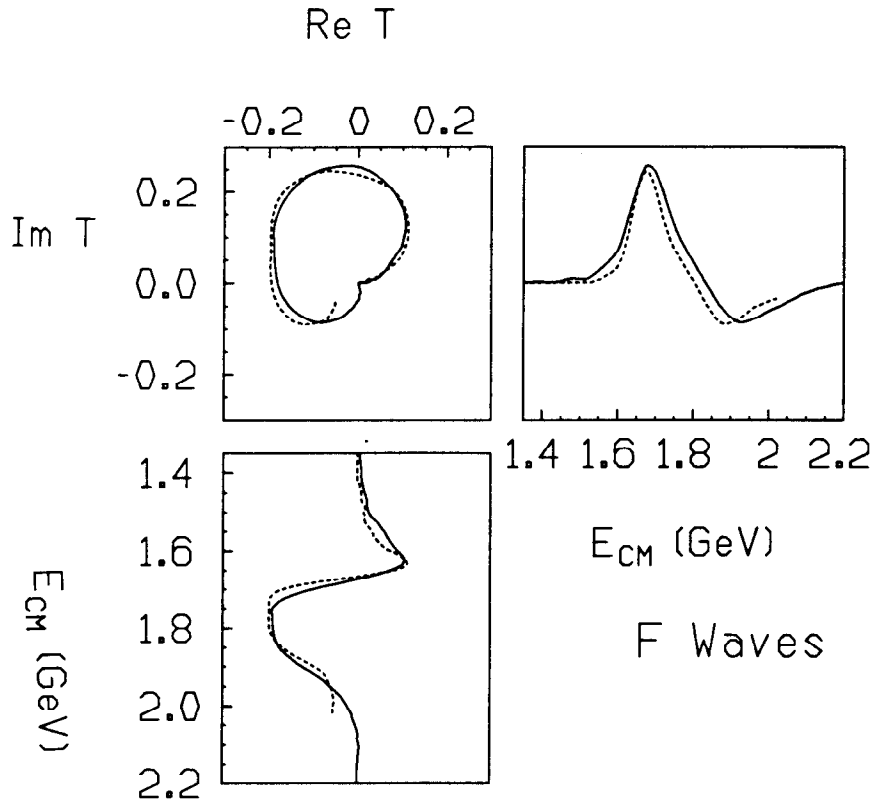


Fig. 11. Test of the prediction for a linear relation between $\pi N \rightarrow \pi N$ and $\bar{K}N \rightarrow \bar{K}N$, Eq. 12. The scattering matrix T is plotted both as function of energy and in $\text{Im}(T)$ vs. $\text{Re}(T)$ representation. Continuous lines: linear combination of the experimental F_{15} and F_{37} $\pi N \rightarrow \pi N$ amplitudes. Dotted lines: linear combination of the experimental F_{05} and F_{17} $\bar{K}N \rightarrow \bar{K}N$ amplitudes. $\bar{K}N$ amplitudes are shifted by the strange quark mass ≈ 150 MeV.

originally done in Ref. 5. In that case there are only 3 reduced amplitudes and no dynamical assumptions are necessary. In order to test the predictions inherent to 3-flavors, it is however necessary to consider relations between strange and non-strange amplitudes.^[17] One such relation reads

$$a_1 F_{15}^{\pi N} + a_2 F_{37}^{\pi N} = b_1 F_{05}^{\bar{K}N} + b_2 F_{07}^{\bar{K}N} \quad (12)$$

where a -s and b -s are purely group-theoretical coefficients obtained from C_i -s in Eq. (11), and $F_{15}^{\pi N}$, $F_{37}^{\pi N}$, $F_{05}^{\bar{K}N}$ and $F_{07}^{\bar{K}N}$ are the experimental partial-wave amplitudes.

As shown by Fig. 11, the prediction contained in Eq. (12) is satisfied with remarkable accuracy. It is also possible to derive similar predictions for G -waves. At present the partial wave analysis for the G -wave $\bar{K}N$ is not yet reliable enough. The G -wave linear relation is therefore a real prediction for what the $\bar{K}N$ G -

waves should look like. I very much hope that this prediction will be put to a test sometime in the near future, perhaps with the advent of the K -factories. It is important to note that Eq.(12) *cannot* be obtained from $SU(3)_f$ by itself. While $SU(3)_f$ is part of the symmetry used to derive Eq. (12), it is clear that $SU(3)_f$ alone cannot produce such a relation, since it mixes amplitudes with different total angular momenta. A more detailed argument shows that even the more elaborate ‘conventional’ symmetries, such as $SU(6)$ are also incapable of reproducing Eq. (12).^[17] . That being the case, the very precise experimental confirmation of the F -wave linear relations should be regarded as another strong testimony in favor of the view that the nucleon indeed can be regarded as a soliton of the meson field.

I hope that this brief review has convinced you that the chiral soliton picture of the nucleon is not only valid on a qualitative basis, but also can be used to study details of low energy hadronic phenomena in a way complementary to and on a par with the quark picture.

REFERENCES

1. E. Witten, *Nucl. Phys.* **B160** (1979) 57.
2. E. Witten, in Lewes Workshop Proc.; A. Chodos *et al.*, Eds; Singapore, World Scientific, 1984.
3. G. Adkins, C. Nappi, and E. Witten, *Nucl. Phys.* **B228**, 552 (1983).
4. M. P. Mattis and M. Karliner, *Phys. Rev.* **D31** (1985) 2833 and references therein.
5. M. P. Mattis and M. Peskin, *Phys. Rev.* **D32** (1985) 58.
6. A. Hayashi, G. Eckart, G. Holzwarth, and H. Walliser, *Phys. Lett.* **147B**, 5 (1984).
7. H. Walliser and G. Eckart, *Nucl. Phys.* **A429**, 514 (1984).
8. M. Karliner and M. P. Mattis, *Phys. Rev. Lett.* **56** (1986) 428.
9. M. Karliner and M. P. Mattis, *Phys. Rev.* **D34** (1986) 1991.
10. M. Karliner and M. P. Mattis, SLAC-PUB-3991, to be published in proceedings of the 2nd Conference on the Interaction Between Particles and Nuclear Physics, Lake Louise, Canada.
11. G. Höhler, F. Kaiser, R. Koch, and E. Pietarinen, *Handbook of Pion-Nucleon Scattering* (Fachinformationszentrum, Karlsruhe, 1979), Physik Daten No. 12-7. Reproduced in Review of Particle Properties, *Rev. Mod. Phys.* **56**, part II (1984). ($\pi N \rightarrow \pi N$)

12. R. E. Cutkosky *et al.*, in *Baryon 1980* (conference proceedings), ed. N. Isgur; reproduced in Review of Particle Properties, *op. cit.* ($\pi N \rightarrow \pi N$)
13. D. M. Manley, R. A. Arndt, Y. Goradia, and V. L. Teplitz, *Phys. Rev. D***30**, 904 (1984). ($\pi N \rightarrow \pi \Delta$)
14. K. Hashimoto, *Phys. Rev. C***29** (1984) 1377. ($KN \rightarrow KN$)
15. R. A. Arndt and L. D. Roper, *Phys. Rev. D***31** (1985) 2230. ($KN \rightarrow KN$)
16. G. P. Gopal *et al.*, *Nucl. Phys. B***119** (1977) 362. Reproduced in Review of Particle Properties, *op. cit.* ($\bar{K}N \rightarrow \bar{K}N$)
17. M. Karliner, *Phys. Rev. Lett.* **57** (1986) 523